Desalination and Water Treatment
www.deswater.com

doi: 10.5004/dwt.2017.21549

99 (2017) 59–71
December

Soil moisture assessment from MODIS data

E. Taktikou[a], G. Papaioannou[a,*], G. Bourazanis[b,c], P. Kerkides[c]

[a]*Department of Physics, National and Kapodistrian University of Athens, University Campus Phys-5 Build., 15784 Zografos, Greece, email: gpapaioa@phys.uoa.gr (G. Papaioannou)*
[b]*Department of Rural Economy and Veterinary of Regional Government of Laconia, Sparta, Laconia 23100, Greece, email: gbourazanis@windtools.gr*
[c]*Department of Natural Resources Development and Agricultural Engineering, Agricultural University of Athens, Iera Odos 75, 11855 Athens, Greece, email: kerkides@aua.gr (P. Kerkides)*

Received 23 November 2016; Accepted 26 May 2017

ABSTRACT

Soil moisture is important for its role in the soil surface energy balance, since it can control the availability of latent heat flux, the crop development and yield production. Assessing soil moisture, even with the recent wide-spread application of the dielectric devices is a time consuming and laborious endeavor. Thus, this study evaluates the capability of soil water content predicted from remote sensing to indicate the soil/canopy water content at short time and space scale, through comparisons with daily soil moisture data determined in situ, using dielectric devices. Daily aqua moderate resolution imaging spectroradiometer normalized difference vegetation index (NDVI) and the diurnal (daytime and nighttime) land surface temperature (DLST) difference are employed to retrieving daily volumetric soil moisture content (θ) at Sparta experimental field, during the growing season (May–October), of the years 2010, 2011, 2012 and 2014. The concept of apparent thermal inertia (ATI), based on the DLST data, is used for estimating the remotely sensed top soil moisture saturation index (SMSI). Daily soil moisture content (θ_{SMSI}) is then obtained from ATI maximum- and minimum-value and the volumetric saturated and residual soil moisture content, θ_{sat} and θ_{res}, respectively, and is compared with the experimental values of volumetric soil moisture content (SM) measured at various depths (10, 20, 30, 40, 60, 80 and 100 cm). Simple relationships are also calibrated between SM and DLST or ATI or NDVI during the years 2010, 2011 and 2014. These are tested for predicting θ (θ_{DLST} or θ_{ATI} or θ_{NDVI}, respectively) during the year 2012. First, θ_{SMSI}, as well as, θ_{ATI} or θ_{DLST} or θ_{NDVI} predict θ satisfactorily, as compared with the measured SM. Hence, they can offer a considerable guidance toward applying a rational and sustainable irrigated agriculture and other related fields. The predictions of θ are also especially tested, during the summer period (June–August) and the obtained results are equally satisfactory.

Keywords: Soil moisture; Apparent thermal inertia; NDVI; Land surface temperature; MODIS data

1. Introduction

Soil moisture is an important parameter in hydrological modeling that influences the energy transfer between the land surface and the atmosphere by controlling the partition of available energy, further affecting the climate. Soil moisture determination is of paramount importance for a rational application of irrigated agriculture, especially in arid or semi-arid regions, where water scarcity and low quality waters may seriously affect crop development and productivity. Despite their reliability, conventional point measurements are complex, labor-demanding, time-consuming and

* Corresponding author.

Presented at the conference on Efficient and Sustainable Water Systems Management toward Worth Living Development, 2nd EWaS 2016, Chania, Greece, June 1–4, 2016.

hence expensive. The recent development and wide-spread application of the so-called dielectric sensors which exploit the amazing feature of water's dielectric constant to be exceptionally high (~80), while all other soil's constituents expose dielectric constant values not larger than 5, made the whole process of SM determination much easier. However, even this methodology cannot be used in large areas, since the spatial and temporal variations of soil properties, terrain and vegetation cover, make the selection of representative field sites difficult. It is in this sense, that remote sensing methodologies are nowadays moving fast to fill this gap. In contrast with the field methods, remote sensing is an effective tool for estimating soil moisture and drought monitoring at various scales, because of large coverage, and multispectral and multitemporal observations from satellite sensors. Although the physical principles upon which the remote sensing prediction of SM values is obtained are well posed, nonetheless there is always the need for their calibration and verification by comparisons with SM values obtained directly from in situ measurements.

Estimating soil moisture from remotely sensed data has covered a wide spectrum ranging from visible to microwave bands. The basis of retrieving soil moisture from microwave remote sensing data is the correlation between soil moisture and dielectric characteristics of the target and radar backscatters [1]. The method can be used either at day or at night and even under cloudy skies due to its penetration capability [2]. Recently, the soil moisture active–passive L-band microwave radiometer has been designed to measure soil moisture with 4% volumetric accuracy at 40 km spatial resolution [3]. Despite the benefits of microwave methods, optical and thermal methods are also fundamental in remote sensing of soil moisture, because of their capability for providing high spatial resolution maps, in particular when compared with spatial resolution (>10 km) available from microwave sensors.

Soil temperature is a key variable in the land surface process, since it affects the energy and water cycle of the land–atmosphere system and it is depended on the soil moisture and vegetation cover. Inversely, a lot of studies have indicated that soil moisture is depended on soil temperature and vegetation status. Thus, at optical and thermal infrared domains, land surface temperature (LST), vegetation index (i.e., NDVI) and albedo could provide information about the condition of soil moisture content. Thermal inertia (TI) is a physical variable describing the impedance of the medium (the soil in this case) to variations of temperature and is defined as $TI = \sqrt{\rho K c}$, where K is soil thermal conductivity (W m^{-1} K^{-1}), ρ is soil bulk density (kg m^{-3}) and c is soil heat capacity (J kg^{-1} K^{-1}). When TI values are high, the variation of temperature is small for a given transfer of heat, while when TI values are low, the variation of temperature is high for the same transfer of heat. In addition, the specific heat capacity of water being equal to 4.18 kJ kg^{-1} K^{-1} is much higher than of dry soil (e.g., 0.8 kJ kg^{-1} K^{-1}) and as a consequence, high soil moisture values lead to high TI values of soil, which result in lower diurnal temperature fluctuation. The research for modeling TI is still an ongoing challenge, focusing mainly in the improvement of its analytical expressions [4–9] or its routinely use, for estimating SM in bare soil and sparsely vegetated areas [4,8,10–12]. Due to the difficulty of measuring ρ, K and c, TI has been approached from the estimations of apparent thermal inertia (ATI), by using remote sensing data, as proposed by Price [4]. Various methods have been referred to estimating SM either based upon ATI [8,13,14] or based upon DLST or NDVI or their combination in the 'triangle method' (developed first by Price [15]) [9,16–18].

This study evaluates the capability of volumetric soil water content predicted from various remote sensing data to indicate the soil/canopy water content at short time and space scale through comparisons with actually measured in situ (by dielectric devices) soil moisture data. Thus, daily aqua moderate resolution imaging spectroradiometer (MODIS) normalized difference vegetation index (NDVI) and the diurnal (daytime and nighttime) land surface temperature (DLST) difference are used to estimating daily volumetric soil moisture content (θ) in an olive orchard at Sparta, during the growing period (May–October), of the years 2010, 2011, 2012 and 2014. Daily θ, based on the concept of TI, is estimated from DLST and the soil moisture saturation index (SMSI) and is compared with the experimental values of volumetric soil moisture content (SM) measured at various depths (10, 20, 30, 40, 60, 80 and 100 cm). Simple relationships between SM and DLST or ATI or NDVI are also calibrated, during the years 2010, 2011 and 2014 and they are tested for predicting θ, during the year 2012.

2. Data and methods

2.1. Data

In this study, soil volumetric water content measurements (SM) taken from an olive orchard at the rural area of Sparta (latitude 37°04′N, longitude 22°05′E and altitude 0.212 km), during the growing season (May–October), of the years 2010, 2011, 2012 and 2014 were used. Soil moisture monitoring tubes had been properly installed, in order to measure SM at 10, 20, 30, 40, 60, 80 and 100 cm depths (SM_{10}, SM_{20}, SM_{30}, SM_{40}, SM_{60}, SM_{80} and SM_{100}, respectively) using the ML2 dielectric device. More details about the collection and monitoring of soil moisture and other soil attributes, as well as information about the irrigation regime and the irrigation water quality being used, can be found in Bourazanis and Kerkides [19,20]. The ML2 theta probe is an impedance sensor with an operating frequency of 100 MHz. It consists of an input–output cable, probe body and a sensing head. The sensing head has an array of four cylindrical rods, 60 mm long and 3 mm in diameter. Three outer rods form a triangle, with the fourth in the center. The outer rods are connected to the instrument ground and form an electrical shield around the central rod, which transmits the signal in continuation from the probe body. The sensing head is inserted into the soil and behaves as an additional section of the internal transmission line of the entire probe body. The ML2 measures the difference in voltage amplitude between the sensor body and the section in the soil, which is dependent on the impedance of the medium between the sensing rods. This single voltage is then related to the soil dielectric constant (ε_s) as:

$$\sqrt{\varepsilon_s} = 1.07 + 6.4V - 6.4V^2 + 4.7V^3 \quad (1)$$

where V is the measured voltage with values between 0 and 1 V (Delta-T Devices Ltd., Cambridge, UK, 2007). This V range

corresponds to an approximate water content between 0 to 0.5 $m^3 m^{-3}$ and to a maximum value of ε_s equal to 33 [21,22]. The volumetric soil moisture (θ) is determined from ε_s by a simple calibration relationship of the form:

$$\theta = c\sqrt{\varepsilon_s} + d \quad (2)$$

where c and d are soil-specific fitting parameters. Detailed descriptions on dielectric sensors calibration and other related issues can be found in Kargas and Kerkides [23,24].

Remotely sensed data obtained by the MODIS, during the growing period of the years 2010, 2011, 2012 and 2014 were also used in this study. The MODIS sensors with spatial resolutions of 250, 500 and 1,000 m, depending on the spectral band, provide 1 day and 1 night image under clear sky conditions. MODIS LST 'represents the radiometric temperature related to the thermal infrared radiation emitted from the land surface observed by an instantaneous MODIS observation' [25,26]. Aqua passes from south to north over the equator at about 1:30 am and 1:30 pm (local solar time) at each day and thus, the daytime and the nighttime LST records represent measurements corresponding to around 1:30 am and 1:30 pm (local solar time). The MYD11A1 MODIS Aqua land product (version 5), was used, which offers daily daytime (LST_{day}) and nighttime (LST_{night}) LST data stored on a 1-km spatial resolution and gridded in the sinusoidal projection [27].

The MODIS product (MYD09GA) data, with band 1 (red wavelength) and band 2 (near-infrared wavelength), were used to calculate daily NDVI at 500 m resolution in the selected station of Sparta, during growing periods of the years 2010, 2011, 2012 and 2014. NDVI represents the combination of its normalized difference formulation and use of the highest absorption and reflectance regions of chlorophyll and was estimated by the following equation [28]:

$$\mathrm{NDVI} = \frac{\mathrm{NIR} - \mathrm{RED}}{\mathrm{NIR} + \mathrm{RED}} \quad (3)$$

where RED and NIR represent the spectral reflectance measurements in the red and near infrared regions, respectively.

2.2. Methods

This study focuses on the estimation of daily soil moisture content from various remote sensing data and the evaluation of the resulting estimates by their comparisons with SM experimental data averaged, as daily means for each depth. In all analyses, the data of 2010, 2011 and 2014 are used for the calibration procedure, while 2012 data are kept for the validation procedure. In the analysis, soil moisture content is estimated, either from the SMSI, expressed as a function of maximum and minimum ATI (based upon DLST), or from DLST or ATI or NDVI by using calibrated predicting equations.

2.2.1. Apparent thermal inertia

TI can be approached from the estimation of ATI, when using remote sensing data. 'Since the Apparent Thermal Inertia (ATI) presents the temporal and spatial variability of soil moisture' [7], the estimation of soil water content in this analysis is based on the reason that high (low) ATI values correspond to maximum (minimum) soil water content. The ATI is estimated according to the following equation [29]:

$$\mathrm{ATI} = C\frac{1 - a_0}{\mathrm{DLST}} \quad (4)$$

where ATI is apparent thermal inertia (K^{-1}), a_0 is the surface albedo, DLST is the diurnal land surface temperature difference (K) estimated as: $DLST = LST_d - LST_n$ (LST_d is daytime land surface temperature (K), LST_n is nighttime land surface temperature (K)) and C is solar correction factor estimated as:

$$C = \sin\vartheta \sin\varphi (1 - \tan^2\vartheta \tan^2\varphi) + \cos\vartheta \cos\varphi \arccos(-\tan\vartheta \tan\varphi) \quad (5)$$

where ϑ is latitude and φ is the solar declination.

In this study, the surface albedo a_0 over the olive trees is taken equal to 0.17 [30].

2.2.2. Estimation of soil moisture content based on apparent thermal inertia and soil moisture saturation index

SMSI is determined as:

$$\mathrm{SMSI} = \frac{\theta - \theta_{res}}{\theta_{sat} - \theta_{res}} \quad (6)$$

where θ is the volumetric soil moisture ($m^3 m^{-3}$) (i.e., $\theta = V_w/V_o$, where V_w represents the volume of water and V_o represents the volume of the soil sample, in which V_w is retained), θ_{res} is the residual volumetric soil moisture ($m^3 m^{-3}$) and θ_{sat} is the volumetric soil moisture ($m^3 m^{-3}$) at saturation. These values are commonly used in empirical, analytical expressions [31,32] of the soil moisture retention curve (SMRC) $\theta = f(H)$, which relates θ with the soil water pressure head, H, and appears to be a fundamental soil hydraulic property. The values of the SMSI curve, as a function of H, which ranges from minus infinity, where $\theta = \theta_{res}$, to zero, where $\theta = \theta_{sat}$, that is, in the interval [0,1] and can be considered as a cumulative probability density function, and its derivative d(SMSI)/dH reveals the soil pore size distribution, directly related to the other fundamental soil hydraulic property, the hydraulic conductivity. SMRCs are usually determined in the laboratory, in disturbed or undisturbed soil samples, using Haines apparatuses or Richards' pressure cells and exhibit the hysteresis phenomenon, where for the same value of H/or θ, an infinite number of θ/or H values are possible, depending on the wetting–drying processes' initiation and evolution [33]. A schematic representation of a typical SMRC is shown in Fig. 1, where the values $\theta = \theta_{sat}$ and $\theta = \theta_{res}$ are shown and the phenomenon of hysteresis is also exhibited.

Based on the rationale that the maximum and minimum value of ATI, derived from remote sensing, correspond to the residual and saturated soil moisture content (θ_{res} and θ_{sat}, respectively), the $SMSI_0$ can be determined as:

$$\mathrm{SMSI}_0 = \frac{\mathrm{ATI} - \mathrm{ATI}_{min}}{\mathrm{ATI}_{max} - \mathrm{ATI}_{min}} \quad (7)$$

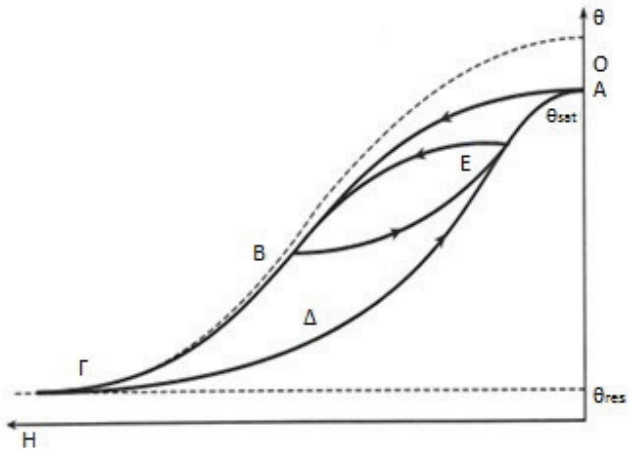

Fig. 1. Schematic representation of the soil moisture retention curve in which the values of θ_{res} and θ_{sat} are shown. The phenomenon of hysteresis, where for the same value of *H*, an infinite number of θ values are possible depending on the drying–wetting procedure initiation and evolution is also exhibited.

Considering that $SMSI_0$ equals to SMSI and combining Eqs. (6) and (7), the soil moisture content θ_{SMSI} is estimated as a linear function of $SMSI_0$:

$$\theta_{SMSI} = SMSI_0 \times (\theta_{sat} - \theta_{res}) + \theta_{res} \quad (8)$$

In this study, ATI_{max} and ATI_{min} are estimated from all the data of the calibration years (2010, 2011 and 2014) and the saturated (θ_{sat}) or the residual (θ_{res}) soil moisture content is determined under laboratory conditions, as equal to 0.415 or 0.119 $m^3\ m^{-3}$, respectively.

2.2.3. Calibration of predicting expressions for soil moisture content based on diurnal land surface temperature difference or normalized difference vegetation index or apparent thermal inertia

A lot of studies have indicated that soil moisture is depended on soil temperature and vegetation status. Therefore, NDVI and LST could provide information about the condition of soil moisture content. Especially, soil moisture and NDVI have been reported as well correlated, during growing periods [34].

Thus, in this study, daily experimental values of SM for each depth and the average value from all depths are linearly regressed with the corresponding DLST or NDVI or ATI. The results from the linear regressions of the form $y = ax$ (determination coefficient (R^2) and slope (a)) are taken into account to form predicting expressions for soil moisture content, as a linear function with zero intercept of ATI or DLST or NDVI (for each depth or the average value from all depths). The predicting expressions are obtained from the data during the growing season (May–October) of the calibration years 2010, 2011 and 2014.

2.2.4. Validation of soil moisture content predictions

The calibrated predicting equations of soil moisture, as a function of DLST or ATI or NDVI, are used for estimating soil moisture (θ_{DLST}, θ_{ATI} and θ_{NDVI}, respectively) for each depth and the average value from all depths, during the year 2012 (validation year). In addition, θ_{SMSI} (based on ATI_{min} and ATI_{max} calculated from the data of the calibration period) is estimated during the year 2012. The estimated soil moisture values (θ_{SMSI}, θ_{DLST}, θ_{NDVI} and θ_{ATI}) are compared with the corresponding values of SM measured at various depths and the average value from all depths. This validation procedure is also extended to the summer period.

The comparisons are evaluated by the results of linear regressions (determination coefficient (R^2) and slope (a)) and 'difference measures' (root mean square error [RMSE], mean bias error [MBE], mean absolute error [MAE] and the new refined index of agreement [RIA]). The indices which measure 'differences' are employed for evaluating the predicting methods, since 'they are trying to identify and quantify the errors, while the determination coefficient represents only the quality of model' [35]. 'The refined index of agreement (RIA) is in general, more rationally related to model accuracy than are other existing indices' [35]. RIA is dimensionless, bounded by –1.0 and 1.0 and is a reformulation of Willmott's index of agreement (IA), which was developed in 1980s. It must be also noticed that 'the average-error measures based on absolute values of differences (like MAE) are, in general, preferable to those based on squared differences, like the RMSE' [36]. The 'difference measures' are determined as:

$$MAE = \frac{1}{n}\sum_{i=1}^{n}\left|P_i - O_i\right| \quad (9)$$

$$MBE = \frac{1}{n}\sum_{i=1}^{n}\left(P_i - O_i\right) \quad (10)$$

$$RMSE = \sqrt{\frac{1}{n}\sum_{i=1}^{n}\left(P_i - O_i\right)^2} \quad (11)$$

$$RIA = 1 - \frac{\sum_{i=1}^{n}\left|P_i - O_i\right|}{2\sum_{i=1}^{n}\left|O_i - \bar{O}\right|} \text{ When: } \sum_{i=1}^{n}\left|P_i - O_i\right| \le 2\sum_{i=1}^{n}\left|O_i - \bar{O}\right| \quad \text{or} \quad (12)$$

$$RIA = \frac{2\sum_{i=1}^{n}\left|O_i - \bar{O}\right|}{\sum_{i=1}^{n}\left|P_i - O_i\right|} - 1 \text{When: } \sum_{i=1}^{n}\left|P_i - O_i\right| > 2\sum_{i=1}^{n}\left|O_i - \bar{O}\right|$$

where P_i is the estimated value by the model and O_i is the observed one.

3. Results

Fig. 2 shows the time evolution of the predicted volumetric soil moisture content (θ_{SMSI}) and the volumetric soil moisture content measured at the depth of 10 cm (SM_{10}) or its average value from all depths (SM_{Av}), during the growing season (May–October) of the calibration years. It is evident that the best agreement exists between θ_{SMSI} and the surface volumetric soil moisture.

Similarly, the time evolution of the DLST difference or the ATI or the NDVI and the experimental values of SM_{10} and SM_{Av} are apparent in Fig. 3 or 4 or 5, respectively, during

the period May–October of the calibration years. In general, the time evolution of SM_{10} or SM_{Av} presents a rather similar pattern with the time evolution of DLST and ATI, while the values of NDVI seem to show a time lag, when they are compared with the corresponding SM_{10} or SM_{Av}.

As a consequence, predicting expressions of soil moisture content for each depth and the average value from all depths are calibrated through the corresponding linear regressions between SM_{10} (or SM_{20} or SM_{30} or SM_{40} or SM_{60} or SM_{80} or SM_{100} or SM_{Av}) and DLST (or ATI or NDVI).

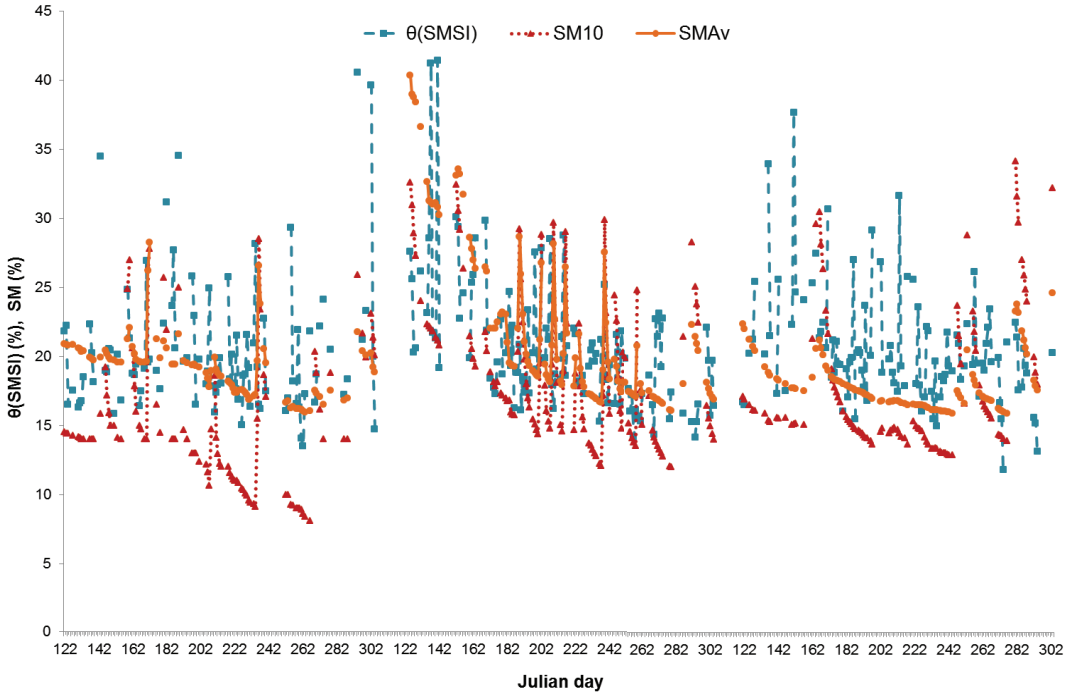

Fig. 2. Time evolution of predicted (by SMSI) volumetric soil moisture content (θ_{SMSI}) and values of volumetric soil moisture content measured at the depth of 10 cm (SM_{10}) or its average value from all depths (SM_{Av}), during the calibration years 2010, 2011 and 2014.

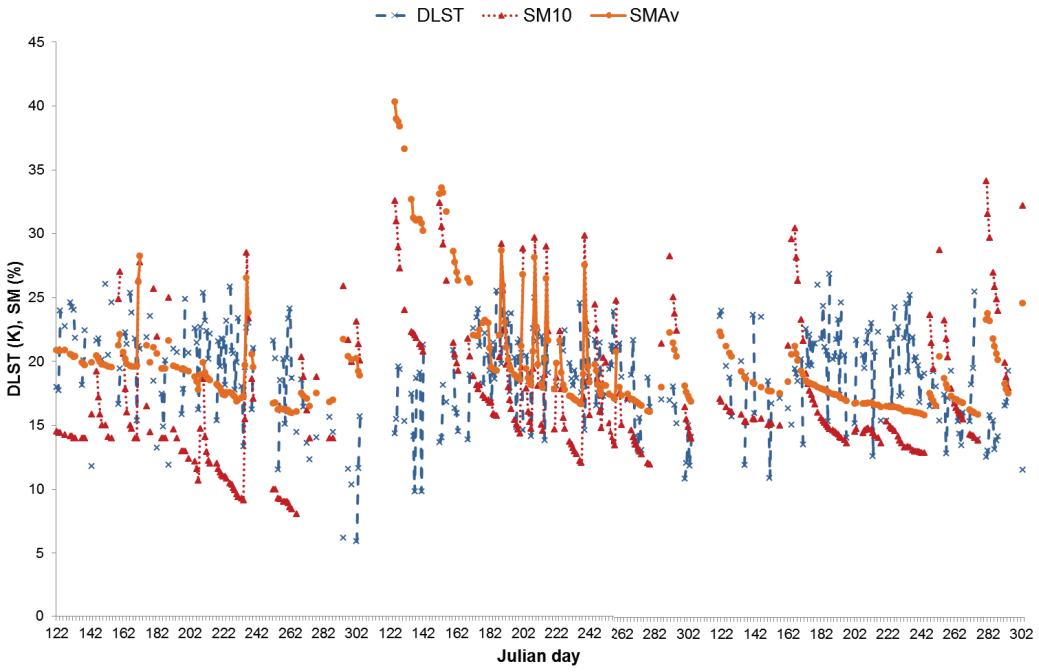

Fig. 3. Time evolution of diurnal land surface temperature (DLST) difference and values of volumetric soil moisture content measured at depths of either 10 cm (SM_{10}) or its average value from all depths (SM_{Av}), during the calibration years 2010, 2011 and 2014.

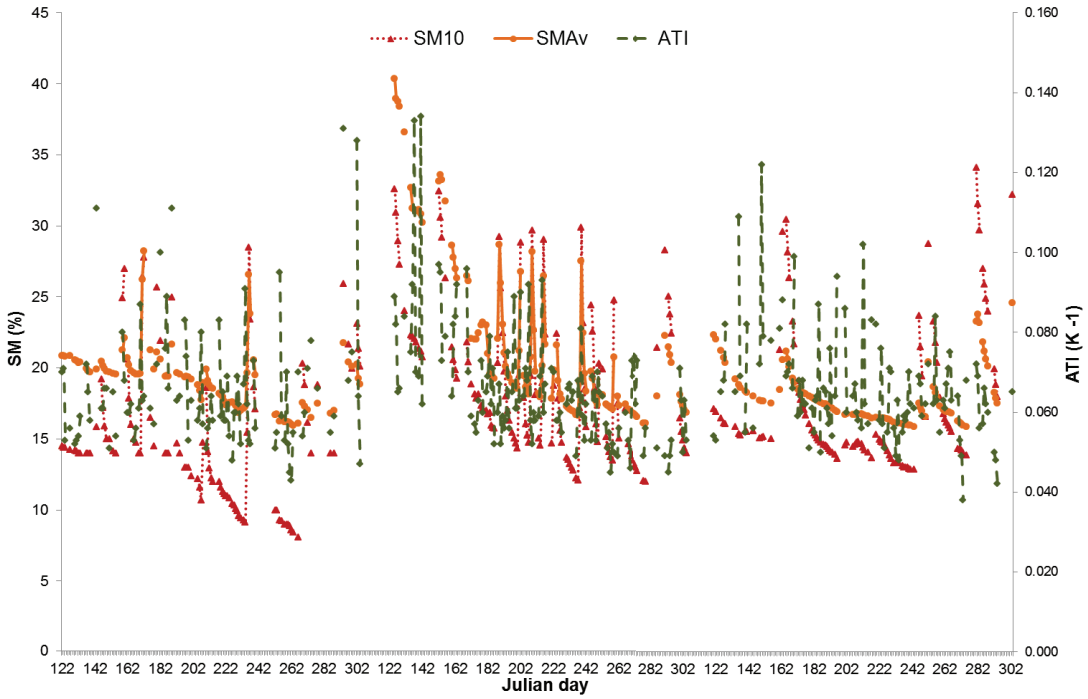

Fig. 4. Time evolution of apparent thermal inertia (ATI) and values of soil moisture content measured at depths of 10 cm (SM_{10}), or its average value from all depths (SM_{Av}), during the calibration years 2010, 2011 and 2014.

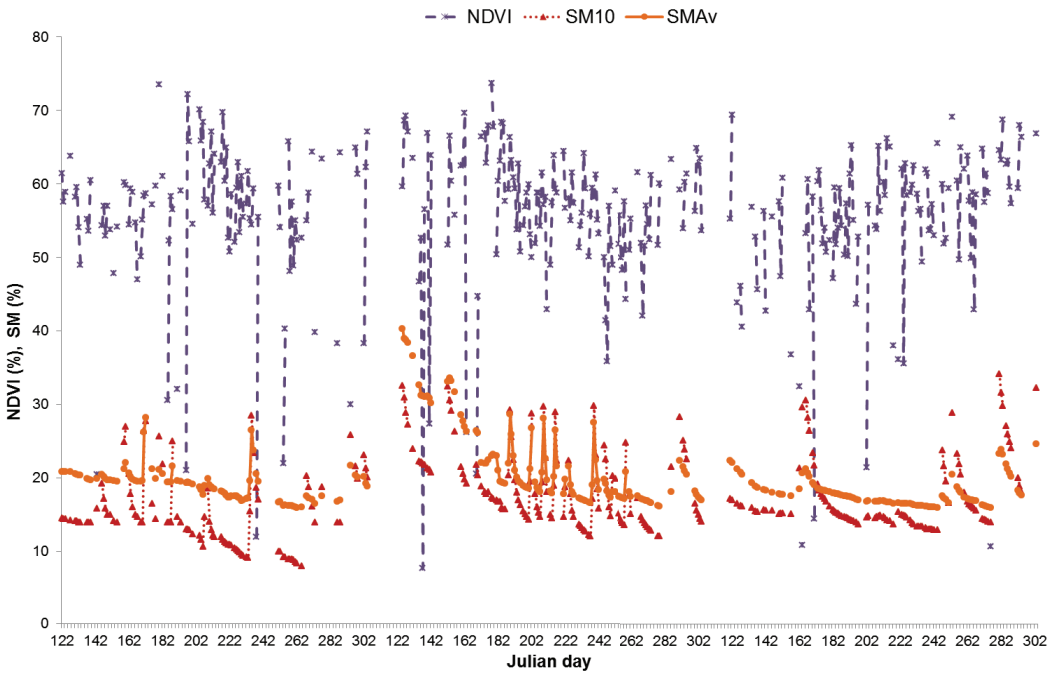

Fig. 5. Time evolution of normalized difference vegetation index (NDVI) and values of soil moisture content measured at depths of 10 cm (SM_{10}), or its average value from all depths (SM_{Av}), during the calibration years 2010, 2011 and 2014.

The results of the linear regressions with zero intercept of the form $y = ax$ (determination coefficient (R^2) and slope (α)) between SM in various depths and DLST or ATI and NDVI, during the growing period are shown in Table 1. All slopes are found statistically significant (at 99.9% confidence level) and the R^2 are quite high in all regressions, including even the ones with NDVI. For example, the linear regressions between SM_{10} and DLST (or ATI or NDVI) resulted in slopes equal to 0.866 (or 253.478 or 0.302, respectively) and R^2 equal to 0.851 (or 0.898 or 0.888, respectively). The linear

Table 1
Results of the linear regressions (determination coefficient [R^2] and slope [α]) between soil moisture (SM) in various depths and diurnal land surface temperature (DLST) difference or apparent thermal inertia (ATI) a normalized difference vegetation index (NDVI), during the growing period

Depth (cm)	R^2	α	R^2	α	R^2	α
	SM against DLST		SM against ATI		SM against NDVI	
10	0.851	*0.866* ± 0.020	0.898	*253.478* ± 4.839	0.888	*0.302* ± 0.006
20	0.889	*0.920* ± 0.018	0.918	*266.503* ± 4.487	0.920	*0.319* ± 0.005
30	0.893	*1.064* ± 0.021	0.925	*308.825* ± 4.960	0.917	*0.368* ± 0.006
40	0.890	*1.003* ± 0.020	0.917	*290.304* ± 4.919	0.904	*0.345* ± 0.006
60	0.931	*1.112* ± 0.017	0.943	*319.207* ± 4.447	0.935	*0.380* ± 0.006
80	0.909	*0.976* ± 0.018	0.931	*298.690* ± 4.327	0.914	*0.334* ± 0.006
100	0.910	*1.089* ± 0.020	0.929	*313.754* ± 4.912	0.916	*0.373* ± 0.007
Average	0.910	*1.004* ± 0.018	0.937	*290.539* ± 4.255	0.928	*0.346* ± 0.006

regressions between SM_{Av} and DLST (or ATI or NDVI) have shown slopes equal to 1.004 (or 290.539 or 0.346, respectively) and R^2 equal to 0.910 (or 0.937 or 0.928, respectively). All the slopes found for the growing period are almost similar, with the ones obtained from the calibrations based upon data of the summer period [37].

All predicted (either by SMSI or by the previously referred predicting equations based on DLST, or ATI or NDVI) soil moisture contents (θ_{SMSI}, θ_{DLST}, θ_{ATI}, θ_{NDVI}, respectively) are compared with the values of SM, measured at various depths and the average value from all depths, during the validation year. The results of their linear regressions (R^2 and *a*) and their 'difference measures' (RMSE, MBE, RIA and MAE) are shown for the growing period in Table 2. Considering the special interest for predicting θ during the summer period, the methods (as calibrated during the growing period) are also evaluated for the period June–August and the results are presented in Table 3.

During the growing period, the comparisons between θ_{SMSI} or θ_{DLST} or θ_{ATI} or θ_{NDVI} and measured SM in various depths show very high values of R^2 (0.92 to 0.97) and very small values of MAE (<4.0% or <5.0% or <4.4% and <4.5%, respectively), at all depths (Table 2). On the contrary, RIA reveals quite large variation at different depths, with the greater values (0.396 or 0.328 or 0.341 and 0.325, respectively) achieved at the depth of 10 cm. Negative RIAs are observed in the comparisons of SM against θ_{DLST} at all depths greater than 20 cm, while they are limited (starting from the depth of 60 cm) in the rest of the comparisons. Thus, focusing on the comparisons revealing important positive RIAs, it seems that MBE is smaller than 6% only when θ_{SMSI} or θ_{DLST} are compared with SM_{10} or SM_{20}, while higher MBEs are observed from the comparisons between θ_{ATI} (or θ_{NDVI}), either with SM_{10} (19% or 20%, respectively) or SM_{20} (12% or 13%, respectively). RMSEs are high, when comparing θ_{SMSI} or θ_{DLST} or θ_{ATI} or θ_{NDVI} either with SM_{10} (28% or 30% or 32% or 34%, respectively) or with SM_{20} (23% or 27% or 24% or 26%, respectively). The measured soil moisture content estimated as average value from all depths (SM_{Av}), seems to be predicted from θ_{SMSI} with a high R^2 (0.963) and small errors (MAE, MBE and RMSE are equal to 2.79%, –1.64% and 19.30%, respectively), although RIA appears to be very small (0.02). SM_{Av} is predicted from θ_{DLST} or θ_{ATI} or θ_{NDVI} with slightly worse R^2 (0.956, 0.963, 0.961, respectively) and slightly greater MAE (4.16%, 3.00%, 2.64%, respectively), MBE (10.73%, –8.17%, –10.17%, respectively) and RMSE (25.36%, 20.15%, 21.17%, respectively). The RIAs are found small, as well. Generally, according to the results of comparisons of θ_{SMSI}, θ_{DLST}, θ_{NDVI} and θ_{ATI} with SM at different depths, an appreciable approximation of experimental values of soil moisture at depth of 10 cm is apparent, while the predictions by θ_{SMSI} are more accurate than θ_{DLST}, θ_{NDVI}, θ_{ATI}. SM_{Av} is roughly predicted by θ_{SMSI} or θ_{DLST} or θ_{ATI} or θ_{NDVI}, with θ_{SMSI}, being the best predictor.

During the summer period, the comparisons between θ_{SMSI} or θ_{DLST} or θ_{ATI} or θ_{NDVI} and measured SM in various depths show very high values of R^2 ranging from 0.91 to 0.98 (Table 3). The MAEs are found small (less than 3.7% or 5.0% or 3.5% or 4.7%, respectively). RIAs are quite different for each depth, being positive only in the comparisons with SM_{10} (0.38 or 0.31 or 0.41 or 0.29), respectively. For the 10 cm depth, the MBEs are equal to 5.7%, or 6.2% or –13.9% or –18.2% and the RMSEs are equal to 26.1%, or 26.7% or 27.6% or 34.1%, respectively. Overall, the values of θ_{SMSI} or θ_{ATI} or θ_{DLST} may predict SM for the 10 cm depth, with θ_{NDVI} being the worst predictor. Additionally, SM_{Av} is roughly predicted from θ_{SMSI}, during summer.

Fig. 6 shows the time evolution of SM_{10}, and the predicted θ_{SMSI} and θ_{ATI} (a) or θ_{DLST} and θ_{NDVI} (b), during the year 2012. Similarly, Fig. 7 shows the time evolution of SM_{Av}, and the predicted θ_{SMSI} and θ_{ATI} (a), θ_{DLST} and θ_{NDVI} (b), during the year 2012. It is evident that θ_{SMSI} and θ_{ATI} have a rather more similar time evolution with SM_{10}, as compared with θ_{DLST} and θ_{NDVI}. The time evolution of SM_{Av} is somehow approached by θ_{SMSI}, but less satisfactorily by θ_{ATI} or θ_{DLST} or θ_{NDVI}. Generally, it is evident that θ_{SMSI} is in a better agreement with SM as compared with θ_{ATI} or θ_{DLST} or θ_{NDVI} and all predictions of θ are in a better agreement with SM_{10}.

4. Discussion

This study evaluates the comparisons of daily soil moisture content estimated from various MODIS remote sensing data (DLST and NDVI) with SM measured at 10, 20, 30, 40, 60, 80 and 100 cm depths and the average value from all depths, at a small temporal and spatial scale. The study focuses on the growing- (or summer-) period, since the best results for

Table 2
Results of the linear regressions (determination coefficient [R^2] and slope [α]) and 'difference measures' (root mean square error [RMSE], mean bias error [MBE], refined index of agreement [RIA] and mean absolute error [MAE]) between predicted (by SMSI or ATI, or DLST or NDVI) soil moisture contents (θ_{SMSI}, θ_{ATI}, θ_{DLST}, θ_{NDVI}, respectively) and values of volumetric soil moisture content (SM) measured at various depths, during the growing period of the validation year

Depth (cm)	R^2	α	RMSE (%)	MBE (%)	RIA	MAE (%)
	θ_{SMSI} against SM					
10	0.928	*0.952* ± 0.025	27.700	–0.118	0.396	4.041
20	0.952	*1.002* ± 0.021	22.935	2.743	0.269	3.076
30	0.956	*0.938* ± 0.019	21.196	–4.566	0.097	3.082
40	0.957	*1.025* ± 0.020	21.497	4.213	0.013	2.497
60	0.967	*0.888* ± 0.015	19.939	–10.618	–0.515	3.409
80	0.961	*1.064* ± 0.020	22.609	7.811	–0.167	2.877
100	0.963	*0.908* ± 0.017	20.249	–8.122	0.080	3.196
Average	0.963	*0.973* ± 0.018	19.292	–1.639	0.018	2.787
	θ_{DLST} against SM					
10	0.916	*0.919* ± 0.026	29.783	–3.013	0.328	4.490
20	0.936	*1.025* ± 0.025	27.309	5.990	0.021	4.116
30	0.946	*1.113* ± 0.025	29.242	13.855	–0.304	4.908
40	0.947	*1.147* ± 0.025	31.241	17.201	–0.388	4.877
60	0.967	*1.108* ± 0.019	23.286	11.446	–0.605	4.180
80	0.960	*1.164* ± 0.022	29.156	17.986	–0.455	4.399
100	0.960	*1.107* ± 0.021	25.262	12.189	–0.210	4.397
Average	0.956	*1.091* ± 0.022	25.360	10.728	–0.318	4.159
	θ_{ATI} against SM					
10	0.927	*0.776* ± 0.020	31.990	–18.646	0.341	4.406
20	0.951	*0.857* ± 0.018	24.415	–12.016	0.216	3.298
30	0.956	*0.931* ± 0.019	21.360	–5.298	0.085	3.124
40	0.957	*0.956* ± 0.019	20.899	–2.781	0.062	2.801
60	0.967	*0.911* ± 0.016	19.200	–8.322	–0.487	3.224
80	0.960	*0.990* ± 0.019	20.297	0.350	–0.067	2.570
100	0.962	*0.915* ± 0.017	20.141	–7.369	0.089	3.166
Average	0.963	*0.909* ± 0.017	20.147	–8.170	–0.054	2.998
	θ_{NDVI} against SM					
10	0.921	*0.760* ± 0.021	33.565	–20.380	0.325	4.511
20	0.944	*0.844* ± 0.019	26.113	–13.490	0.250	3.152
30	0.957	*0.916* ± 0.018	21.284	–7.298	0.181	2.796
40	0.958	*0.939* ± 0.018	20.801	–5.096	0.140	2.567
60	0.964	*0.894* ± 0.016	20.248	–10.348	–0.399	2.749
80	0.960	*0.942* ± 0.018	20.143	–4.951	0.054	2.267
100	0.960	*0.897* ± 0.017	21.223	–9.543	0.182	2.841
Average	0.961	*0.892* ± 0.017	21.168	–10.168	0.070	2.638

predicting SM from remote sensing data have been referred generally, during this period [34]. Furthermore, the olive orchard at Sparta has been selected, as a representative sample of bare soil and sparsely vegetated region, for applying the ATI concept [4,8,11,12].

The evaluation of the resulting predictions based upon θ_{SMSI} indicates that there is a reasonably good agreement of the experimental values of soil moisture averaged, as daily means for the depth of 10 cm (Tables 2 and 3). Especially, SM_{10} is predicted quite accurately, either during the growing period (RIA = 0.40, MAE = 4.04%, MBE = –0.12%, RMSE = 27.70% and R^2 = 0.93), or the summer period (RIA = 0.38, MAE = 3.64%, MBE = 5.72%, RMSE = 26.10% and R^2 = 0.94). θ_{SMSI} may also predict SM_{20}, rather satisfactorily (as compared with SMs at the other depths), during the growing season (RIA = 0.27, MAE = 3.08%, MBE = 2.74%, RMSE = 22.94% and R^2 = 0.95). The measured soil moisture content estimated as average value from all depths seems

Table 3
Results of the linear regressions (determination coefficient [R^2] and slope [α]) and 'difference measures' (root mean square error [RMSE], mean bias error [MBE], refined index of agreement [RIA] and mean absolute error [MAE]) between predicted (by SMSI or ATI, or DLST or NDVI) soil moisture contents (θ_{SMSI}, θ_{ATI}, θ_{DLST}, θ_{NDVI}, respectively) and values of volumetric soil moisture content (SM) measured at various depths, during the summer period of the validation year

Depth (cm)	R^2	α	RMSE (%)	MBE (%)	RIA	MAE (%)
	θ_{SMSI} against SM					
10	0.941	*1.016* ± 0.031	26.100	5.719	0.384	3.638
20	0.965	*1.060* ± 0.024	21.248	7.446	–0.041	2.709
30	0.972	*1.005* ± 0.021	17.152	0.923	–0.425	2.361
40	0.973	*1.101* ± 0.022	20.853	10.403	–0.652	2.518
60	0.977	*0.922* ± 0.017	16.235	–7.834	–0.800	2.866
80	0.961	*1.057* ± 0.026	21.740	12.976	–0.789	2.519
100	0.964	*0.898* ± 0.021	15.698	–3.254	–0.577	2.508
Average	0.966	*0.992* ± 0.022	16.858	3.290	–0.436	2.329
	θ_{DLST} against SM					
10	0.938	*1.017* ± 0.031	26.675	6.237	0.316	4.036
20	0.968	*1.130* ± 0.025	24.588	14.708	–0.304	3.733
30	0.981	*1.243* ± 0.021	29.806	24.604	–0.721	4.867
40	0.982	*1.283* ± 0.021	33.204	28.494	–0.828	5.081
60	0.983	*1.189* ± 0.019	24.621	18.928	–0.868	4.357
80	0.961	*1.157* ± 0.028	32.686	27.952	–0.892	4.907
100	0.962	*1.095* ± 0.026	27.596	22.254	–0.775	4.713
Average	0.967	*1.117* ± 0.028	26.333	20.333	–0.688	4.213
	θ_{ATI} against SM					
10	0.940	*0.827* ± 0.025	27.635	–13.917	0.415	3.455
20	0.965	*0.907* ± 0.021	19.864	–8.018	0.004	2.588
30	0.971	*0.997* ± 0.021	17.179	0.121	–0.431	2.387
40	0.972	*1.027* ± 0.021	17.142	2.966	–0.599	2.186
60	0.976	*0.945* ± 0.018	15.737	–5.494	–0.787	2.690
80	0.961	*0.984* ± 0.024	17.126	5.124	–0.742	2.059
100	0.964	*0.905* ± 0.021	15.844	–2.491	–0.577	2.508
Average	0.966	*0.926* ± 0.021	16.092	–3.599	–0.441	2.348
	θ_{NDVI} against SM					
10	0.907	*0.778* ± 0.030	34.102	–18.221	0.292	4.718
20	0.945	*0.863* ± 0.025	25.183	–12.208	–0.058	2.757
30	0.962	*0.950* ± 0.023	19.637	–4.867	–0.404	2.275
40	0.962	*0.975* ± 0.023	19.545	–2.436	–0.592	2.145
60	0.963	*0.898* ± 0.021	20.307	–10.290	–0.777	2.569
80	0.962	*0.915* ± 0.022	19.109	–3.346	–0.723	1.916
100	0.962	*0.866* ± 0.021	19.330	–7.571	–0.529	2.253
Average	0.960	*0.885* ± 0.022	20.921	–8.458	–0.442	2.352

to be roughly predicted from θ_{SMSI}, during the growing season. The R^2 is high (0.96), the errors are small (MAE = 2.79%, MBE = –1.64%) or reasonable (RMSE = 19.29%), but the estimated RIA is quite small (0.02). These results are similar and rather slightly better, as compared with the results obtained for 10 sites in Europe [13] (R^2 or RMSE range in the interval [0.54, 0.88] or [3.9%, 35.7%], respectively) or for 8 sites in China [14] (R^2 ranges from 0.17 to 0.85). The prediction of SM_{20} and SM_{Av} from θ_{SMSI} seems to be slightly worse, during summer (Table 3).

The evaluation of all predictions shows that θ_{SMSI} is the best predictor, but θ_{DLST}, θ_{ATI} and θ_{NDVI} may also predict SM_{10}, rather satisfactorily, during the growing season (Table 2). The estimated RIA, MAE and R^2 are of the same order, as the ones obtained for the θ_{SMSI} predictions, but RMSE is higher (29.78%, 31.99% and 33.57%, respectively) and MBE is higher in θ_{ATI} and θ_{NDVI} predictions (–18.65% and –20.38%). It seems that the experimental values of SM_{10} may be approached quite satisfactorily by simple parameters such as the DLST and the ATI (which incorporates as extra parameter, only the surface

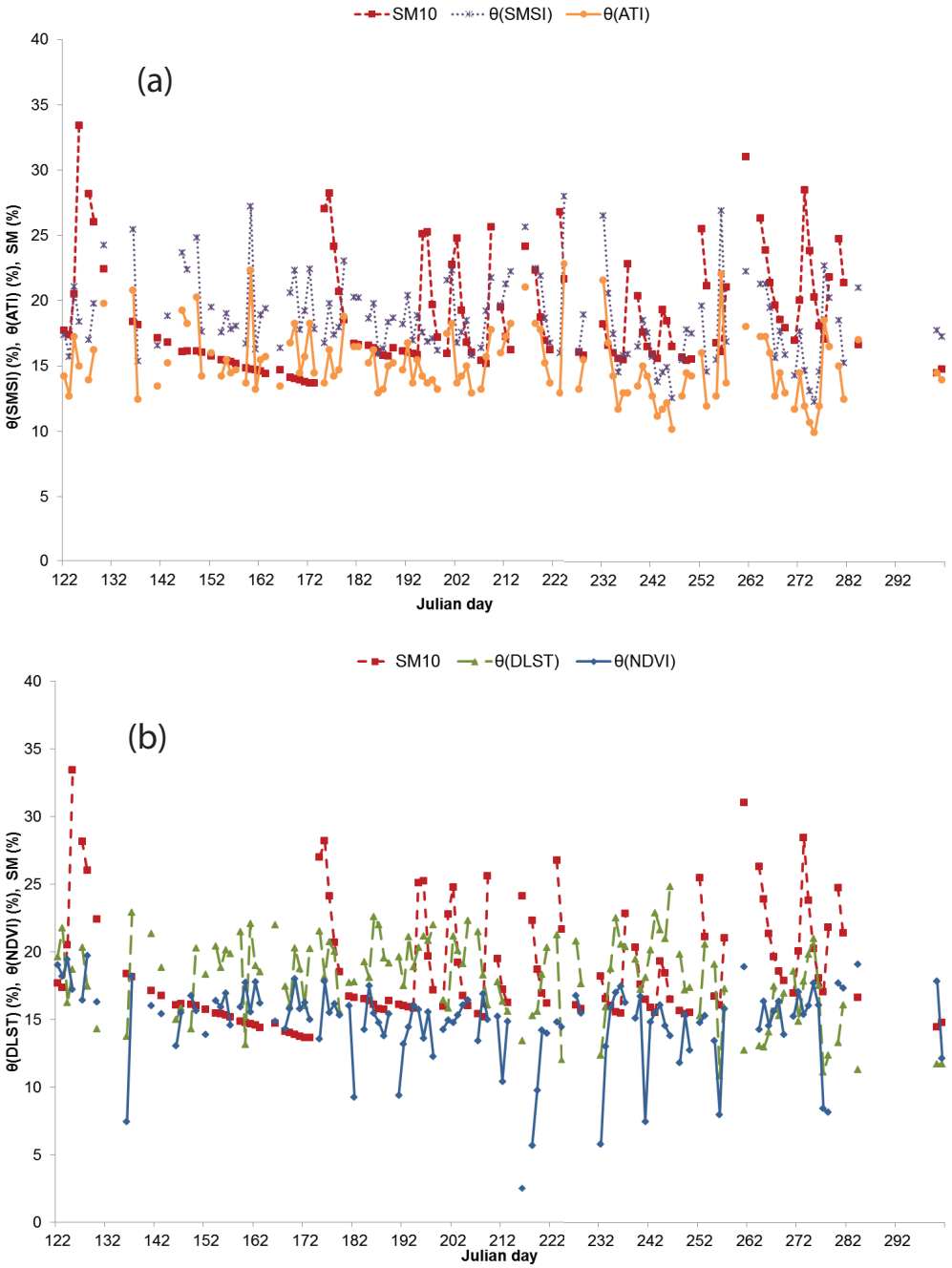

Fig. 6. Time evolution of the experimental values of volumetric soil moisture content measured at depth of 10 cm (SM_{10}) and predicted by SMSI and ATI (a), or DLST and NDVI (b), soil moisture contents (θ_{SMSI} and θ_{ATI} or θ_{DLST} and θ_{NDVI}, respectively), during the validation year 2012.

albedo), although the latent heat, the sensible heat and other atmospheric parameters on the surface, are not considered. It must be mentioned that Zhenhua and Yingshi [9] reported predictions by ATI worse than the ones estimated by their model of TI, which was improved by taking into account the effect of vegetation. They also suggested the depth of 20 cm, as the most appropriate for estimating SM, although most of researchers consider calibrations at each depth. A possible prediction of SM by DLST and ATI was already apparent from the high values of the determination coefficients estimated from the linear regressions between SM at each depth and either DLST or ATI, during the calibration years (Table 1). High R^2 (ranging from 0.89 to 0.94) were also obtained from the linear regressions between SM and NDVI at each depth, although a time lag of NDVI was apparent, as compared with SM time evolution (Fig. 5). The latter can be attributed on one hand to increasing NDVI when SM is increasing, during the growing period and on the other hand to the 16-d composition of the daily NDVI (i.e., the 16-d average is the average of the current day and the following 15 d). It has already been reported by Wang and Xie

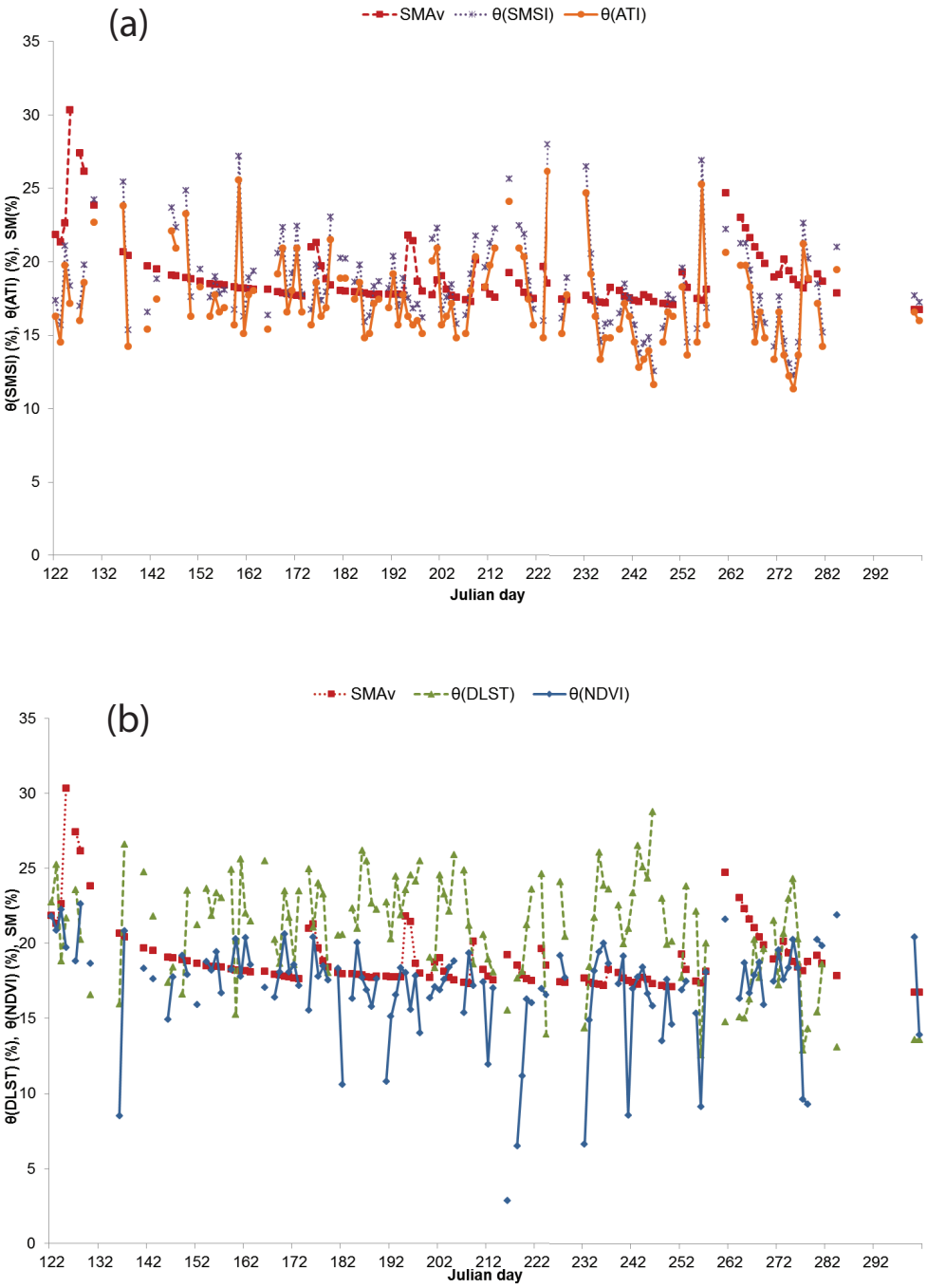

Fig. 7. Time evolution of the experimental values of volumetric soil moisture content as its average value from all depths (SM_{Av}) and predicted by SMSI and ATI (a), or DLST and NDVI (b), soil moisture contents (θ_{SMSI} and θ_{ATI} or θ_{DLST} and θ_{NDVI}, respectively), during the validation year 2012.

[16] that 'R between NDVI and soil moisture peaks when NDVI has 0–5 day time lag over measured soil moisture in a semi-arid climate'. The results from the evaluation of NDVI employed to predicting SM are quite reasonable (Table 2), as compared with the results (R^2 ranging from 0.33 to 0.77) referred in Schnur et al. [38] when using 'deseasonalized time series of soil moisture and deseasonalized time series of NDVI with a 5-day time lag'. The results are also better than those estimated from the correlations between SWAT simulated soil moisture and NDVI, during the leaf falling period of three kinds of forest (R^2 varied from 0.55 to 0.62). Moreover, θ_{DLST}, θ_{ATI} and θ_{NDVI} verify roughly the experimental values of SM_{20} and less satisfactorily the values of SM_{Av}, during the growing or summer period.

5. Conclusions

This study focuses on the estimation of daily soil moisture content from MODIS remote sensing data, during the

growing- (or summer-) period. The evaluation of all resulting predictions, indicate that there is an appreciable proximity of the experimental values of soil moisture averaged, as daily means for the depth of 10 cm.

More analytically, θ_{SMSI} seems to predict quite accurately SM_{10}, either during the growing period, or the summer period, as compared with θ_{DLST}, θ_{ATI} and θ_{NDVI}. θ_{SMSI} may also predict SM_{20}, rather satisfactorily, during the growing season. SM_{Av} seems to be roughly predicted from θ_{SMSI}, during the growing season. The prediction of SM_{20} and SM_{Av} from θ_{SMSI} is rather slightly worse, during summer.

The evaluation of all predictions shows that θ_{SMSI} is the best predictor, but θ_{DLST}, θ_{ATI} and θ_{NDVI} may also predict SM_{10}, rather satisfactorily, during the growing- (or summer-) period. Moreover, θ_{DLST}, θ_{ATI} and θ_{NDVI} verify roughly the experimental values of SM_{20} and less satisfactorily the values of SM_{Av}, during the growing- (or summer-) period.

Acknowledgment

The Greek Ministry of Rural Development and Food and the former Prefecture of Laconia for funding the project are duly acknowledged.

References

[1] E.G. Njoku, J.A. Kong, Theory for passive microwave remote sensing of near-surface soil moisture, J. Geophys. Res., 82 (1977) 3108–3118.
[2] E.G. Njoku, D. Entekhabi, Passive microwave remote sensing of soil moisture, J. Hydrol., 184 (1996) 101–129.
[3] J.R. Piepmeier, P. Focardi, K.A. Horgan, J. Knuble, N. Ehsan, J. Lucey, C. Brambora, P.R. Brown, P.J. Hoffman, R.T. French, R.L. Mikhaylov, E.-Y. Kwack, E.M. Slimko, D.E. Dawson, D. Hudson, J. Peng, P.N. Mohammed, G. De Amici, A.P. Freedman, J. Medeiros, F. Sacks, R. Estep, M.W. Spencer, C.W. Chen, K.B. Wheeler, W.N. Edelstein, P.E. O'Neill, E.G. Njoku, SMAP L-band microwave radiometer: instrument design and first year on orbit, IEEE Trans. Geosci. Remote Sens., 55 (2017) 1954–1966.
[4] J.C. Price, On the analysis of thermal infrared imagery: the limited utility of apparent thermal inertia, Remote Sens. Environ., 18 (1985) 59–73.
[5] Y. Xue, A.P. Cracknell, Advanced thermal inertia modelling, Int. J. Remote Sens., 16 (1995) 431–446.
[6] J.A. Sobrino, M.H. El Kharraz, Combining afternoon and morning NOAA satellites for thermal inertia estimation: 2 methodology and application, J. Geophys. Res., 104 (1999) 9455–9465.
[7] T. Yu, G.L. Tian, The application of thermal inertia method the monitoring of soil moisture of north china plain based on NOAA-AVHRR data, J. Remote Sens., 1 (1997) 24–31.
[8] V. Tramutoli, P. Clamps, M. Marella, N. Pergola, C. Sileo, Feasibility of Hydrological Application of Thermal Inertia from Remote Sensing, Second Plinius Conference on Mediterranean Storms, 2000 October 16–18, Siena, Italy, DIFA-Contrada Macc, Potenza.
[9] L. Zhenhua, Z. Yingshi, Research on the method for retrieving soil moisture using thermal inertia model, Sci. China, Ser. D, 49 (2006) 539–545.
[10] H.A. Pohn, T.W. Offield, K. Watson, Thermal inertia mapping from satellite discrimination of geologic units in Oman, J. Res. US Geol. Surv., 22 (1974) 147–158.
[11] A.B. Kahle, A.R. Gillespie, A.F.H. Goetz, Thermal inertia imaging: a new geologic mapping tool, Geophys. Res. Lett., 3 (1976) 26–28.
[12] A. Verhoef, Remote estimation of thermal inertia and soil heat flux for bare soil, Agric. For. Meteorol., 123 (2004) 221–236.
[13] W. Verstraeten, F. Veroustraete, C.J. van der Sande, I. Grootaers, J. Feyen, Soil moisture retrieval using thermal inertia, determined with visible and thermal spaceborne data, validated for European forests, Remote Sens. Environ., 101 (2006) 299–314.
[14] F. Veroustraete, Q. Li, W. Verstraeten, X. Chen, A. Bao, Q. Dong, T. Liu, P. Willems, Soil moisture content retrieval based on apparent thermal inertia for Xinjiang province in China, Int. J. Remote Sens., 33 (2012) 3870–3885.
[15] J.C. Price, Using spatial context in satellite data to infer regional scale evapotranspiration, IEEE Trans. Geosci. Remote Sens., 28 (1990) 940–948. doi:10.1109/36.58983.
[16] X. Wang, H. Xie, Different responses of MODIS-derived NDVI to root-zone soil moisture in semi-arid and humid regions, J. Hydrol., 340 (2007) 12–24.
[17] R.R. Gillies, W.P. Kustas, T.N. Carlson, J. Cui, K.S. Humes, A verification of the 'Triangle' method for obtaining surface soil water content and energy fluxes from remote measurements of the normalized difference vegetation index (NDVI) and surface temperature, Int. J. Remote Sens., 18 (1997) 3145–3166. doi: 10.1080/014311697217026.
[18] J.Y. Park, S.R. Ahn, S.J. Hwang, C.H. Jang, G.A. Park, S.J. Kim, Evaluation of MODIS NDVI and LST for indicating soil moisture of forest areas based on SWAT modeling, Paddy Water Environ., 12 (2014) S77–S88.
[19] G. Bourazanis, P. Kerkides, Evaluation of Sparta's Municipal Wastewater Treatment Plant's Effluent as an Irrigation Water Source According to Greek Legislation, Water is Necessary for Life (Win4life), International Conference Proceedings, 2015, Tinos.
[20] G. Bourazanis, P. Kerkides, Evaluation of Sparta's municipal wastewater treatment plant's effluent as an irrigation water source according to Greek Legislation, Desal. Wat. Treat., 53 (2015) 3427–3437.
[21] G. Kargas, P. Kerkides, Performance of the THETA PROBE ML2 in the presence of nonuniform soil water profiles, Soil Tillage Res., 103 (2009) 425–432.
[22] G. Kargas, P. Kerkides, M.S. Seyfried, Response of three soil water sensors to variable solution electrical conductivity in different soils, Vadose Zone J., 13 (2014). doi:10.2136/vzj2013.09.0169.
[23] G. Kargas, P. Kerkides, Water content determination in mineral and organic porous media by ML2 THETA PROBE, Irrig. Drain., 57 (2008) 435–449.
[24] G. Kargas, P. Kerkides, Evaluation of a dielectric sensor for measurement of soil water electrical conductivity, J. Irrig. Drain. Eng., 136 (2010) 553–558.
[25] Z. Wan, New refinements and validation of the MODIS land-surface temperature/emissivity products, Remote Sens. Environ., 112 (2008) 59–74.
[26] E.E. Maeda, D.A. Wiberg, P.K.E. Pellikka, Estimating reference evapotranspiration using remote sensing and empirical models in a region with limited ground data availability in Kenya, Appl. Geogr., 31 (2011) 251–258.
[27] K. Wang, Z. Wan, D. Wang, M. Sparrow, J. Liu, X. Zhou, S. Haginova, Estimation of surface long wave radiation and broadband emissivity using MODIS land surface temperature/ emissivity products, J. Geophys. Res., 110 (2005) D11109.
[28] C.J. Tucker, Red and photographic infrared linear combinations for monitoring vegetation, Remote Sens. Environ., 8 (1979) 127–150.
[29] D.S. Mitra, T.J. Majumdar, Thermal inertia mapping over the Brahmaputra basin, India using NOAA-AVHRR data and its possible geological applications, Int. J. Remote Sens., 225 (2004) 3245–3260.
[30] C. Cammalleri, C. Agnese, G. Ciraolo, M. Minacapilli, G. Provenzano, G. Rallo, Actual evapotranspiration assessment by means of a coupled energy/hydrologic balance model: Validation over an olive grove by means of scintillometry and measurements of soil water contents, J. Hydrol., 392 (2010) 70–82.
[31] M.Th. van Genuchten, A closed-form equation for predicting the hydraulic conductivity of unsaturated soils, Soil Sci. Soc. Am. J., 44 (1980) 892–898.
[32] R.H. Brooks, A.T. Corey, Hydraulic Properties of Porous Media, Hydrology Papers, no 3, Colorado State University, Fort Collins, Colorado, 1964.

[33] A. Poulovasilis, Hysteresis of pore water, an application of the concept of independent domains, Soil Sci., 93 (1962) 405–412.
[34] T.J. Farrar, S.E. Nicholson, A.R. Lare, The influence of soil type on the relationships between NDVI, rainfall, and soil moisture in semiarid Botswana: II. NDVI response to soil moisture, Remote Sens. Environ., 50 (1994) 121–133.
[35] C.J. Willmot, Some comments on the evaluation of model performance, Bull. Am. Meteorol. Soc., 63 (1982) 1309–1313.
[36] C.J. Willmott, S.M. Robesonb, K. Matsuura, A refined index of model performance, Int. J. Climatol., 32 (2012) 2088–2094.
[37] E. Taktikou, G. Bourazanis, G. Papaioannou, P. Kerkides, Prediction of soil moisture from remote sensing data, Proc. Eng., 162 (2016) 309–316.
[38] M.T. Schnur, H. Xie, X. Wang, Estimating root zone soil moisture at distant sites using MODIS NDVI and EVI in a semi-arid region of southwestern USA, Ecol. Inf., 5 (2010) 400–409.